

Temperature-insensitive refractive index sensing by use of micro Fabry–Pérot cavity based on simplified hollow-core photonic crystal fiber

Ying Wang,^{1,2} D. N. Wang,^{1,*} C. R. Liao,¹ Tianyi Hu,¹ Jiangtao Guo,³ and Huifeng Wei³

¹Department of Electrical Engineering, The Hong Kong Polytechnic University, Hong Kong, China

²Laboratory of Optical Information Technology and School of Science, Wuhan Institute of Technology, Wuhan 430073, China

³State Key Laboratory of Optical Fiber and Cable Manufacture Technology, Yangtze Optical Fibre and Cable Company Ltd. R&D center, Wuhan 430073, China

*Corresponding author: eednwang@polyu.edu.hk

Received November 16, 2012; revised December 21, 2012; accepted December 21, 2012;
posted December 21, 2012 (Doc. ID 179987); published January 16, 2013

A temperature-insensitive micro Fabry–Pérot (FP) cavity based on simplified hollow-core (SHC) photonic crystal fiber (PCF) is demonstrated. Such a device is fabricated by splicing a section of SHC PCF with single mode fibers at both cleaved ends. An extremely low temperature sensitivity of ~ 0.273 pm/°C is obtained between room temperature and 900°C. By drilling vertical micro-channels using a femtosecond laser, the micro FP cavity can be filled with liquids and functions as a sensitive refractometer and the refractive index sensitivity obtained is ~ 851.3 nm/RIU (refractive index unit), which indicates an ultra low temperature cross-sensitivity of $\sim 3.2 \times 10^{-7}$ RIU/°C. © 2013 Optical Society of America

OCIS codes: 060.5295, 060.2370, 120.0120.

Optical fiber refractive index (RI) sensors have a broad range of applications in chemical, biomedical, and environmental monitoring, due to their small size, high sensitivity and fast response time. To date, most of optical fiber RI sensors are based on fiber Bragg grating (FBG) [1], long-period fiber grating (LPFG) [2,3], Fabry–Pérot (FP) or Mach–Zehnder interferometer [4,5], micro-fiber [6], selectively infiltrated photonic crystal fiber (PCF) coupler [7,8] and many other interesting structures [9–11].

The FBG based RI sensor generally presents a low sensitivity on the order of ~ 100 nm/RIU (refractive index unit), and the FBG should be fabricated in an exposed-core fiber or a microfiber. It has been reported that LPFG can provide a sensitivity as high as 1500 nm/RIU [3]. However, LPFG typically exhibits large temperature cross-sensitivity and nonlinear response to the surrounding RI. An ultra-high sensitivity, of up to 24,373 nm/RIU, is achieved by use of a highly birefringent microfiber loop [6]. By employing selective infiltration techniques of PCFs [7,12,13], embedded coupler, modal interferometer, and photonic band-gap structures can be fabricated, which exhibit even higher RI sensitivity such as 38,000 nm/RIU [8]. However, such a sensor can only use the liquids with a RI higher than that of silica (~ 1.46). To operate at around 1.33 of RI, a liquid-filled PCF sensor based on four-wave mixing has been demonstrated, with a high sensitivity of 8800 nm/RIU, however, a large length of PCF (~ 1 m) has to be used [11].

A key issue that existed in the above mentioned configurations is temperature cross-sensitivity because it limits the sensor reliability. One of the solutions to this issue is the use of fiber-optical FP cavity as it exhibits very low temperature sensitivity of ~ 1 pm/°C, due to the small thermo-expansion coefficient of silica. Recently, the micro FP cavity has received increased research attention because of its low temperature cross-sensitivity, high RI and/or strain sensitivities, and convenient

reflection mode of detection. The FP cavity fabricated by focused ion beam milling has been used to measure the RI around 1.30 with a high sensitivity of 1731 nm/RIU [14] however; the temperature cross-sensitivity of the device was not reported. By employing a femtosecond laser, micro FP cavity can be fabricated in single mode fiber (SMF) [15,16] and PCF [17], with a temperature sensitivity of larger than 2 pm/°C, corresponding to a temperature cross-sensitivity of greater than 2×10^{-6} RIU/°C. By splicing a section of hollow-core PCF [18] or Er-doped fiber [19] with SMFs, strain sensors have been demonstrated, with further reduced temperature sensitivity of ~ 0.81 and 0.65 pm/°C, respectively.

In this Letter, we demonstrate a micro FP cavity based on simplified hollow-core (SHC)-PCF for RI sensing with extremely low temperature cross-sensitivity. The device is fabricated by fusion splicing both ends of a section of SHC-PCF with SMFs. The RI sensitivity obtained is ~ 851.3 nm/RIU, with a temperature sensitivity of ~ 0.273 pm/°C. This indicates a temperature cross-sensitivity of only $\sim 3.2 \times 10^{-7}$ RIU/°C, which is lower than that of the previously reported micro FP cavities and other types of fiber-optical RI sensors.

SHC-PCF is composed of a big hollow core and one layer of air-hole cladding, which is proposed by Gérôme *et al.* [20] and Wu *et al.* [21] and shows similar guidance properties as the Kagomé-lattice PCF. The SHC-PCF used in our experiment is manufactured by YOFC Ltd., and the

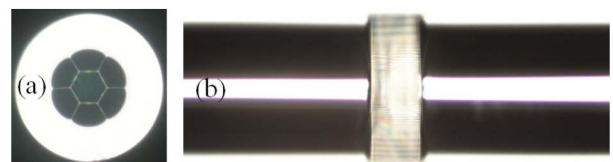


Fig. 1. (Color online) (a) Cross-section view of the SHC-PCF and (b) microscopic image of a micro FP cavity based on SHC-PCF with the cavity length of ~ 48 μm .

diameters of the hexagonal core, the air-hole cladding, and the whole fiber are ~ 29 , 73 , and 140 μm , respectively. The thickness of the silica struts is estimated to be ~ 400 nm. Figure 1(a) is the cross-section view of the SHC-PCF, which has a similar transmission property as that reported in [21]. The micro FP cavity was fabricated by using a conventional fiber cleaving and fusion splicing technique while avoiding any air-hole collapsing [22]. Figure 2(a) shows the microscopic image of a SHC-PCF based micro FP cavity with the length of ~ 48 μm . Such a cavity length can be controlled accurately by use of a microscope during the cleaving process.

A broadband light source was used to connect the micro FP cavity via a 3 dB coupler to observe its reflection spectrum by use of an optical spectrum analyzer (OSA). Figure 2 shows the reflection spectra of the micro FP cavities with lengths of 27, 50, and 75 μm , respectively. The 27 μm long FP cavity exhibits a free spectral range of ~ 47.2 nm, while that of the 50 μm long and 75 μm long cavities are 24.3 and 16.2 nm, respectively, around the wavelength of 1550 nm. The fringe visibilities are larger than 10 dB, which indicates a reasonably good quality of interference fringe pattern of the two light beams reflected by the end facets of SMFs at both splicing joints.

Since the typical temperature sensitivity of micro FP cavities is on the order of 1 $\text{pm}/^\circ\text{C}$, the measurements conducted from room temperature to $\sim 100^\circ\text{C}$ would exhibit large errors due to the OSA resolution of larger than 10 pm. Much broader temperature range should be swept to accurately determine the temperature sensitivity of the micro FP cavity. Thus, we put the 75 μm long FP cavity into a high temperature furnace with an accuracy of 1°C for the thermal stability test. After removing the fiber coatings, the device was heated to 1000°C and maintained there for 2 h, and no obvious deterioration was found in the reflection spectrum. Following a cooling down of the device to the room temperature, the furnace was gradually warmed up to 100°C and subsequently from 100°C to 900°C with a step of 100°C , and the device stayed for 30 min at each step. Then the device was cooled down to room temperature again, following the same procedure as that used in the heating process. The reflection spectra recorded in the cooling procedure was found to coincide with that in the heating process.

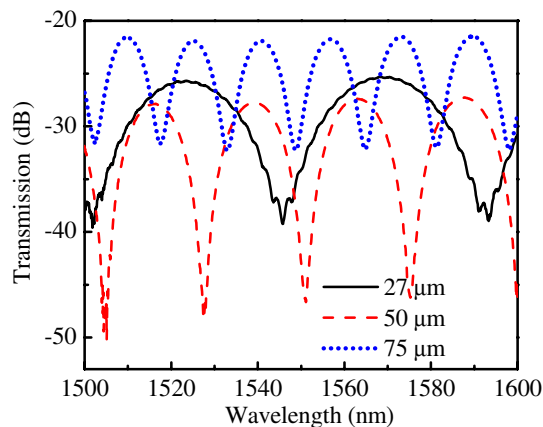


Fig. 2. (Color online) Reflection spectra of the micro FP cavities based on SHC-PCF with cavity lengths of 27, 50, and 75 μm , respectively.

Such a thermal test was repeated four times with reproducible results.

The thermal induced shift of an interference dip around 1550 nm at room temperature for a 75 μm long FP cavity was plotted in Fig. 3, and a temperature sensitivity of ~ 0.273 $\text{pm}/^\circ\text{C}$ was obtained by use of a linear fit of the experimental data. Such temperature sensitivity is even lower than the theoretical value of ~ 0.85 $\text{pm}/^\circ\text{C}$, calculated according to the coefficient of thermal expansion of fused silica ($5.5 \times 10^{-7}/^\circ\text{C}$), which is around 1550 nm. This may be due to the shrinkage of the SHC-PCF fiber core during the heating process. With the temperature increasing, the SHC-PCF would simultaneously expand axially and transversely, and the central air hole might be squeezed and shrunk by the transversal expansion. The decrease of SHC-PCF core diameter would lead to the reduction of the effective index of the core mode, and hence partially cancel out the effect of the micro FP cavity length increasing.

With the knowledge of low temperature sensitivity of the device, a 50 μm long SHC-PCF based FP cavity was constructed to measure the RI of water at different temperatures. Four symmetrically distributed micro-holes were drilled in the middle part of the PCF with a Ti:sapphire femtosecond laser from the fiber surface to the core to allow water to fill in. The micro-holes were fabricated by 2 μJ pulses (800 nm center wavelength, 120 fs pulse duration, and 1 kHz repetition rate) focused with a $20\times$ objective ($\text{NA} = 0.50$) and exhibited the diameter of ~ 5 μm . Then the device was immersed into a water cell and the reflection spectra at different temperatures were recorded. Figure 4(a) shows the reflection spectra of the 50 μm long FP cavity at 30°C , 55°C , and 80°C . The fringe visibilities are beyond 15 dB and their dips shift to the shorter wavelengths with the increase of temperature, as the RI of water is decreased when the water is warmed up. By tracing the fringe dip around 1550 nm, the dip wavelength was recorded and plotted with RI of water at different temperatures [23], as shown in Fig. 4(b). An RI sensitivity of ~ 851.3 nm/RIU can be obtained by linear fitting of the experimental data. Thus the temperature cross-sensitivity of the SHC-PCF based FP cavity can be estimated as $\sim 3.2 \times 10^{-7}$ $\text{RIU}/^\circ\text{C}$.

It should be noted that the SHC-PCF supports the propagation of several modes in the air core, where mode

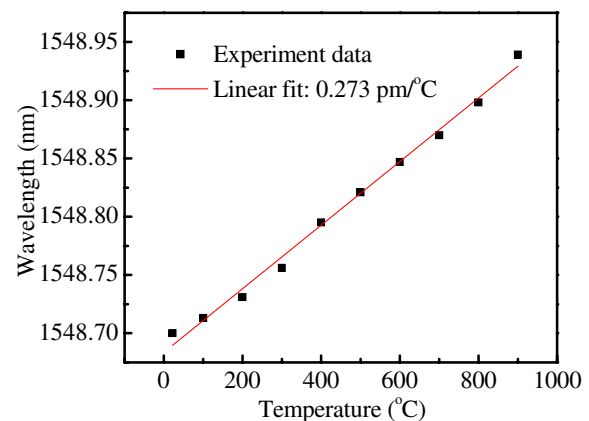


Fig. 3. (Color online) Fringe dip wavelength shift of a 75 μm -long SHC-PCF based FP cavity with temperature variation.

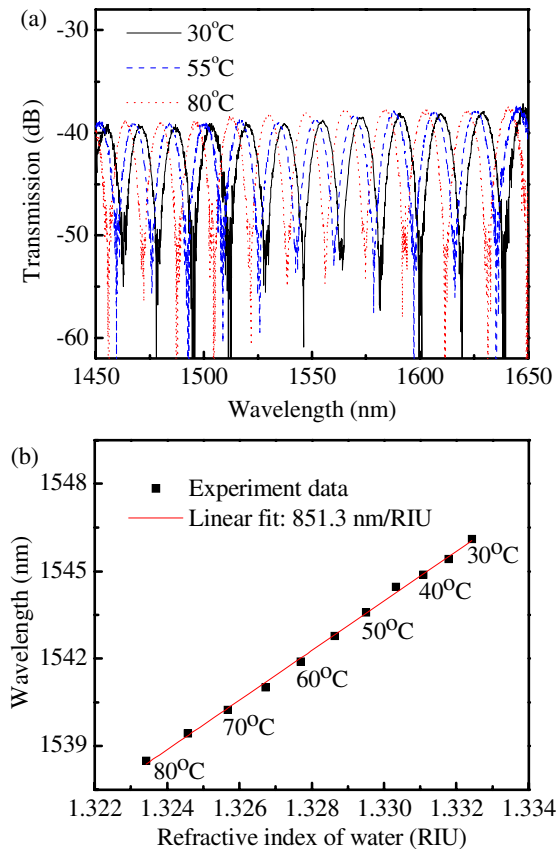


Fig. 4. (Color online) (a) Reflection spectra and (b) fringe dip wavelengths of a 50 μm long FP cavity filled with water at different temperatures.

characteristics can hardly be changed by temperature benefitting from the extremely low thermo-optic coefficient of air. This enables the fabrication of other types of sensors with very low temperature sensitivity, such as LPFGs, which have been proved to be with a temperature sensitivity down to 0.59 pm/°C [21].

In conclusion, we have demonstrated a micro FP cavity interferometer with extremely low temperature sensitivity of ~ 0.273 pm/°C. The micro FP cavity was fabricated by splicing both ends of a section of SHC-PCF with SMFs. The RI sensitivity obtained is ~ 851.3 nm/RIU, which indicates an ultra low temperature cross-sensitivity of $\sim 3.2 \times 10^{-7}$ RIU/°C. The sensors proposed have high potential in chemical and biomedical sensing, and in environmental monitoring.

This work was supported by The Hong Kong Polytechnic University research grant 4-ZZE3, and the National Natural Science Foundation of China under grant no. of 61108016.

References

1. W. Liang, Y. Huang, Y. Xu, R. K. Lee, and A. Yariv, *Appl. Phys. Lett.* **86**, 151122 (2005).
2. D. W. Kim, F. Shen, X. Chen, and A. Wang, *Opt. Lett.* **30**, 3000 (2005).
3. L. Rindorf and O. Bang, *Opt. Lett.* **33**, 563 (2008).
4. H. Y. Choi, G. Mudhana, K. S. Park, U. C. Paek, and B. H. Lee, *Opt. Express* **18**, 141 (2010).
5. Y. Wang, M. Yang, D. N. Wang, S. Liu, and P. Lu, *J. Opt. Soc. Am. B* **27**, 370 (2010).
6. L. Sun, J. Li, Y. Tan, X. Shen, X. Xie, S. Gao, and B. O. Guan, *Opt. Express* **20**, 10180 (2012).
7. D. K. C. Wu, B. T. Kuhlmeier, and B. J. Eggleton, *Opt. Lett.* **34**, 322 (2009).
8. W. Yuan, G. E. Town, and O. Bang, *IEEE Sens. J.* **10**, 1192 (2010).
9. R. Slavík, J. Homola, J. Čtyroky, and E. Brynda, *Sens. Actuators B Chem.* **74**, 106 (2001).
10. V. P. Minkovich, J. Villatoro, D. Monzón-Hernández, S. Calixto, A. B. Sotsky, and L. I. Sotskaya, *Opt. Express* **13**, 7609 (2005).
11. M. H. Frosz, A. Stefani, and O. Bang, *Opt. Express* **19**, 10471 (2011).
12. Y. Wang, C. R. Liao, and D. N. Wang, *Opt. Express* **18**, 18056 (2010).
13. F. Wang, W. Yuan, O. Hansen, and O. Bang, *Opt. Express* **19**, 17585 (2011).
14. W. Yuan, F. Wang, A. Savenko, D. H. Petersen, and O. Bang, *Rev. Sci. Instrum.* **82**, 076103 (2011).
15. T. Wei, Y. Han, Y. Li, H. L. Tsai, and H. Xiao, *Opt. Express* **16**, 5764 (2008).
16. C. R. Liao, T. Y. Hu, and D. N. Wang, *Opt. Express* **20**, 22813 (2012).
17. Y. J. Rao, M. Deng, D. W. Duan, X. C. Yang, T. Zhu, and G. H. Cheng, *Opt. Express* **15**, 14123 (2007).
18. M. S. Ferreira, J. Bierlich, J. Kobelke, K. Schuster, J. L. Santos, and O. Frazão, *Opt. Express* **20**, 21946 (2012).
19. Y. Gong, Y. J. Rao, Y. Guo, Z. L. Ran, and Y. Wu, *IEEE Photon. Technol. Lett.* **21**, 1725 (2009).
20. F. Gérôme, R. Jamier, J. L. Auguste, G. Humbert, and J. M. Blondy, *Opt. Lett.* **35**, 1157 (2010).
21. Z. Wu, Z. Wang, Y. Liu, T. Han, S. Li, and H. Wei, *Opt. Express* **19**, 17344 (2011).
22. L. Xiao, M. S. Demokan, W. Jin, Y. Wang, and C. L. Zhao, *J. Lightwave Technol.* **25**, 3563 (2007).
23. P. Schiebener, J. Straub, J. M. H. Levelt Sengers, and J. S. Gallagher, *J. Phys. Chem. Ref. Data* **19**, 677 (1990).